

Deep Learning Image-based Design of Graphene-reinforced Polyurethane Foams

Alemayehu Admasu*, Devesh Upadhyay†, Rachel Couvreur
Janice Tardiff, Alper Kiziltas, Patrick Blanchard

Research and Advanced Engineering
Ford Motor Company, Dearborn, MI 48124

Abstract

Artificial Intelligence techniques have been rapidly progressing in the past decade and have become an important tool for discovery within the scientific community. The adoption of these techniques within the material science community has been critical in enabling high throughput research through rapid characterization and discovery of materials. Machine (Deep-) learning techniques are being used not only for characterizing materials but also for extrapolating structure-property relationships as well as for generating new structures from existing material structure data. We discuss two case studies where we demonstrate the use of deep learning techniques for modeling and optimizing the design of graphene-reinforced polyurethane (PU) foams. Specifically we demonstrate both forward and inverse design techniques through the use of image regression and Generative Adversarial Networks applied to SEM images of graphene-reinforced polyurethane foams. The dataset and analysis further opens up a wide application of AI for the microstructural studies of PU foams.

Introduction

While Artificial Intelligence (AI) has had major successes in fields such as computer vision, natural language processing (NLP) and autonomous driving to name a few, AI approaches are still in their infancy when applied to materials science (Himanen et al. 2019). The application of AI to material science problems is an emerging area of active research, primary directions including the use of AI techniques for better understanding of material properties, accelerated material discovery and efficient development of advanced materials. In contrast to the traditional trial-and-error approach to material discovery, AI enabled methods offer the promise of a much reduced turnaround time for material discovery and commercialization of novel materials. This has also been demonstrated by (Hiszpanski et al. 2020) where they show that NLP techniques can extract material synthesis insights from scientific literature and predict synthesis parameters and outcomes on new materials systems, vastly outperforming heuristic strategies. Other examples of AI techniques applied to material science include AI-

based screening and experimental validation of thermoplastic polymers (Wu et al. 2019), inorganic phosphor host materials for solid-state lighting (Zhuo et al. 2018), and high-entropy alloys for structural applications (Rickman et al. 2020).

While AI methods require substantially more data than conventional methods, material scientists have traditionally worked with small datasets that are also noisy and sparse. AI based techniques such as data augmentation, transfer learning (Jha et al. 2019), generative models (Schwalbe-Koda and Gómez-Bombarelli 2020), physics informed neural networks (PINNs) (Pun et al. 2019) along with fast sensing and data acquisition systems (Stein and Gregoire 2019) are necessary to alleviate the severe data bottleneck problem. Embedding physics within neural network models guarantees that symmetries and conservation laws, present in the physical system being studied, are not violated in the models. Physics aware AI models also improve computational efficiency and prediction accuracy. Data efficiency in the inverse design can also leverage recent advances in molecular design and optimization (Gómez-Bombarelli et al. 2018; Yang et al. 2020).

In most AI models, the way inputs are transformed into outputs are often opaque resulting in black box solutions (Holm 2019; Iwasaki et al. 2019; Xie and Grossman 2018). As such, to increase the transparency and robustness of AI models for scientific users, interpretability and explainability have become key criteria in model development. Some techniques are Grad-CAM (Selvaraju et al. 2017) which produces coarse localization heatmaps highlighting the important regions in the image used for the predictions and an ablation study where, by removing some “feature” of the model or algorithm, one quantifies the effects on model performance.

In this study, we implemented an integrated approach that combines material science experimentation and artificial intelligence techniques. In particular we use deep learning (DL) methods of image regression and generative adversarial networks (GANs) to provide mechanistic and physical insights from multi-modal, in-situ characterization data and SEM microstructure images. These methods are applied for accelerating material discovery and optimizing physical properties in graphene-reinforced polyurethane foam composites.

*aadmasu@ford.com

†dupadhya@ford.com

Table 1: A summary of the tests and their standards.

Test	Standard
Compression Force Deflection	ASTM D3574 Test C
Compression Modulus	ASTM D3574 Test C
Tensile Stress at Maximum Load	ASTM D3574 Test E
Tensile Modulus	ASTM D3574 Test E
Tear Resistance	Ford Specification WSS-M15P20-B1, 3.3.5

Table 2: Polyurethane foam materials and formulations summary.

Component	Type	Weight Percentage
Petroleum Polyol	Voranol 4701	62.2 %
Cell Opener	Lumulse POE (26) GLYC	0.6%
Surfactant	Tegostab B4690	0.3%
Cross Linker	Diethanolamine (DEA)	0.9%
Catalyst	NiAx A300	0.4%
Catalyst	NiAx A1	0.2%
Blowing Agent	Deionized Water	1.9%
Diisocyanate	Rubinate 7304	33.5%
Additive	Graphene	(0, 0.01, 0.025, 0.05)%

Materials Synthesis and Characterization

Polyurethane (PU) foams are a well-known class of polymers with a wide variety of automotive applications including seat cushions, headliners, engine covers etc. due to their excellent mechanical properties, lightweight nature, high levels of acoustic dampening, thermal stability and reduced cost to name a few (Zachary D. 2019). The customizable nature and versatility of PU foams such as in the choice of catalysts, fillers, isocyanate component, and nature of degree of cross-linking sites, polyol molecular weight, viscosity, etc. has led to the development of various polyurethane materials tailored to meet specific industry needs. Recent studies (Alasti Bonab, Moghaddas, and Rezaei 2019; Kucheyev et al. 2006; Luo et al. 2017) have shown changes in foam microstructural features such as cell size, density, morphology, etc. accompany enhancement in mechanical, electrical, and thermal properties. By synthesizing PU foams reinforced with varied amounts of graphene, we aim to develop here, an image-based AI solution for foam material design and property prediction from SEM images and physical property multi-modal data, as well as, generate realistic synthetic microstructure images based on user-input physical/processing parameters.

PU foam samples were synthesized by reacting polyols with isocyanate in a lab scale production. The polyol is first combined with a few additives including a cell opener, a surfactant, a crosslinker, two catalysts, and a blowing agent before reacting with a diisocyanate. The reader is referred to (Zachary D. 2019) for the detailed synthesis conditions, preparation, and mixing of the polyols and additives. The PU foams were cut to comply with ASTM standard testing procedures to obtain physical and mechanical properties of each foam formulation. The PU foam samples were analyzed based on mechanical testing. Density was measured, and tensile, tear, and compression properties were tested using an Instron 3366 machine. Six samples were selected and

tested from each foam formulation. A summary of the tests and their standards are summarized in Table 1¹. Glass transition temperature and storage modulus were examined using DMA. Three foam samples were analyzed at 10 Hz and 1% strain using Rheometric Scientific Dynamic Mechanical Thermal Analyzer IV.

Deep learning methods for images frequently require datasets in the order of thousands of images. However, a careful selection of labelled images, data augmentation and pre-designed prototypical neural networks can reduce the amount of data needed. Here we mainly implement geometric data augmentation techniques that include rotation, flips, etc. as the properties of the SEM images under study are invariant to these operations.

Image Regression for Physical Properties

Material science image data processing and analysis often require prior subject matter expertise and are labor and time intensive. Recently, various techniques leveraging computer vision and machine learning techniques have been implemented as an efficient alternative for high throughput study of microstructural data such as in (Gola et al. 2018). Herein we implement a state-of-the-art AI based image regression technique to predict the amount of GNP (Graphene Nanoplatelets) additive (wt %) and selected mechanical properties of tensile stress and tensile modulus, based solely on given SEM images of GNP-reinforced PU foams. The mechanical properties of PU foams can vary with changes in foam cell microstructure such as cell size, density, surface morphology and texture which in turn are correlate to their physical properties.

As such scanning electron microscope (SEM) images of the top surface of the above synthesized foams (c.f. Table 2) were obtained using JEOL JSM-6610 scanning elec-

¹Parenthesis indicates standard deviation.

Table 3: Polyurethane foam mechanical and thermal test results data.

Measured Property	Units	0%	0.01%	0.025%	0.05%
Mechanical					
Comp. Stress @ 25% strain	kPa	2.794 (0.163)	3.965 (0.632)	3.889 (0.225)	4.151 (0.569)
Comp. Stress @ 50% strain	kPa	4.102 (0.252)	6.520 (1.201)	7.182 (0.515)	7.109 (1.178)
Comp. Stress @ 65% strain	kPa	6.178 (0.407)	10.957 (2.885)	13.030 (1.832)	12.247 (2.894)
Comp. Modulus	MPa	0.0309 (0.0018)	0.0565 (0.0218)	0.0676 (0.0180)	0.0736 (0.0076)
Tensile Stress @Max Load	kPa	117.97 (6.400)	77.450 (6.402)	88.675 (15.863)	105.325 (38.298)
Tensile Modulus	MPa	0.197 (0.029)	0.190 (0.020)	0.200 (0.005)	0.227 (0.033)
Tear Resistance	N/mm	0.502 (0.045)	0.512 (0.040)	0.539 (0.026)	0.508 (0.070)
Thermal					
Tg	°C	-41.633 (1.293)	-40.805 (2.794)	-43.250 (1.964)	-43.480 (0.078)
Tg Max Point	°C	0.375 (0.023)	0.438 (0.022)	0.374 (0.031)	0.372 (0.028)
SM at RT	Pa	114,340 (1,2200)	98,600 (12,500)	123,440 (24,000)	144,923 (23,400)
SM at Tg	Pa	581,496 (85,900)	935,327 (129,000)	962,087(384,000)	1,545,173 (599,000)

tron microscope instrument at Ford Research and Advanced Engineering. The SEM images were taken under SE2 secondary electron detector at fixed beam energy and working distance. . The brightness and contrast levels were held constant across all images and samples; see also Table 3 . We collected 200 grayscale SEM images from four samples with varied amounts of additive (Control, 0.01%, 0.025%, 0.05%) as shown in Table 4. The SEM data acquisitions specifications include high resolution fixed depth of focus, SED mode with high magnification (25x, approx. 10.3 pix/micron). The resulting dataset was augmented by geometric operations of rotation, flips etc and physical property data were measured for each sample.

	Additive%	Tensile Stress(kPa)	Tensile Modulus(MPa)	Additive%	Tensile Stress(kPa)	Tensile Modulus(MPa)
Ground-truth	0.05%	94.78	0.20	0.025%	112.40	0.21
Predicted	0.049%	94.54	0.19	0.024%	112.80	0.21

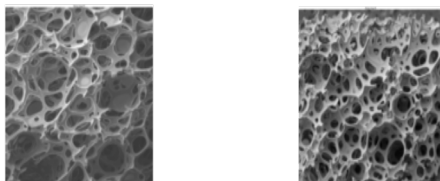


Figure 1: GNP-PU foam SEM image regression of additive percentage and mechanical properties.

We consider an end-to-end deep learning (DL) image regression technique with raw SEM image pixels as input and a supervised training procedure using the mechanical measurements as labels of the SEM images. The DL image regression technique comprises a ResNet34 network (He et al. 2016) pretrained on ImageNet (Krizhevsky, Sutskever, and Hinton 2012) using a PyTorch implementation. The SEM images are normalized with respect to ImageNet stats and the number of outputs is set to three corresponding to additive %, tensile stress and tensile modulus. The loss function is chosen to be mean-squared error loss (MSE) and the model is trained for 100 iterations with resulting R-squared greater than 0.98 for each of the outputs.

The performance of the model is tested by predicting ad-

ditive % and tensile properties on previously unseen examples (20% of the dataset) as shown in Fig. 1. Even though the model currently can be a black-box solution, it performs with high accuracy. The mechanism and explainability of the model shall be investigated further as in (Liu et al. 2020) to gain previously unknown insights or for other materials applications such as in multi-functional polymer composite materials design.

Synthesizing Microstructures from Experimental Parameters: GANs for Inverse Materials Design

In the previous section, we implemented an image regression method where given an SEM image of a material sample, we are able to accurately predict material attributes such as the mechanical performance or graphene additive percent. In this section we implement a generative model that outputs a hypothetical SEM image corresponding to a given material attribute such as synthesis/processing condition or physical properties. This can significantly help domain scientists visualize and understand how changes in material attributes, synthesis/processing conditions impact the sample microstructure features which in turn determine its mechanical, thermal and electrical properties. This is all done without actually performing tests in the lab as well as to discover materials with optimal target properties through investigation of counterfactual relationships (Liu et al. 2020) (i.e. determining material features that control changes in the prediction).

Specifically, we use an image editing generative adversarial network, AttGAN (He et al. 2019), to synthesize realistic SEM images by varying a synthesis parameter, e.g. graphene additive weight percent. Different from other types of GANs which generate images starting from a noise vector, AttGAN is trained on input images along with the attributes encoding the desirable changes, thus reducing the heavy computational resources requirement during training as well as amount of image data. The reader is referred to the original work on AttGAN (He et al. 2019) for details on model architecture. As shown in Figure 2, the AttGAN

Table 4: SEM image dataset summary for GNP-reinforced PU foam.

Samples (GNP-reinforced Foam)	SEM Image Dataset Size
Control (0.0%)	50
0.01%	50
0.025%	50
0.05%	50

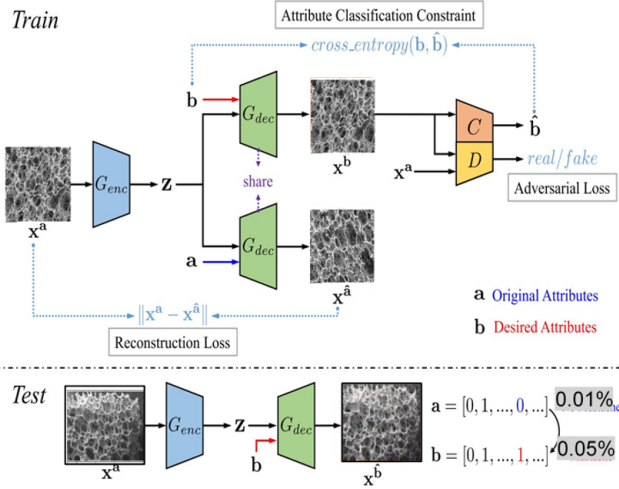


Figure 2: AttGAN model architecture for synthesizing microstructures with specified additive percentage attributes, adapted from (He et al. 2019).

contains three main components at training, i.e. the attribute classification constraint (correct attribute manipulation on the generated image), the reconstruction learning (preserving the attribute-excluding details) and the adversarial learning (for visually realistic generation). The overall objective function for the encoder and decoder (G_{enc}, G_{dec}) shown in the figure is formulated as below,

$$\min_{G_{enc}, G_{dec}} \mathcal{L}_{enc, dec} = \lambda_1 \mathcal{L}_{rec} + \lambda_2 \mathcal{L}_{cls_g} + \mathcal{L}_{adv_g}, \quad (1)$$

while the objective function for the discriminator and the attribute classifier (D, C) is formulated as below,

$$\min_{D, C} \mathcal{L}_{dis, cls} = \lambda_3 \mathcal{L}_{cls_c} + \mathcal{L}_{adv_d}, \quad (2)$$

with λ_1, λ_2 and λ_3 are the hyperparameters for balancing the losses. We trained the AttGAN in the PyTorch implementation with the following model hyperparameters compared to the original implementation: learning rate of 0.002, batch size of 32, number of epochs = 60; for the Generator: attribute loss weight = 10.0; reconstruction loss weight = 100.0; for the Discriminator: gradient penalty weight = 10.0; attribute loss weight = 1.0 and using an Adam optimizer. The results of the training are shown in Fig. 3 where a realistic visualization of the SEM image appearance of the material and subtle effect of the synthesis parameter change is shown given the previously unseen image (from the 20% of the dataset) for 0.01 % graphene additive reinforced PU foam. This can be further extended to demonstrate

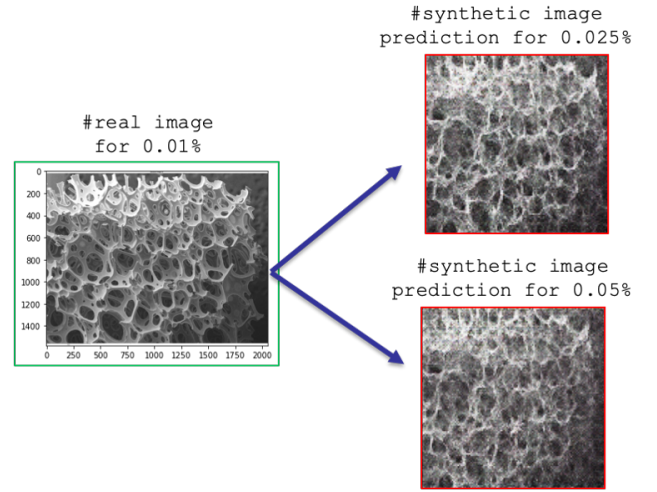


Figure 3: Synthetic image generation of SEM foam microstructure based on varied additive percentages; scale units in μm .

attribute/property-driven image generation process so as to design materials with target optimal properties such as high peak tensile modulus etc.

Conclusion

We demonstrated that state-of-the-art machine learning and deep learning techniques can be leveraged to model and optimize the design of graphene-reinforced polyurethane foams. A deep-learning image regression technique is used to predict mechanical properties of various graphene-reinforced polyurethane foams (PU) based solely on scanning electron microscopy (SEM) images with image regression $R^2 \sim 0.99$. An image editing generative adversarial network, AttGAN, in the PyTorch implementation was implemented to generate realistic synthetic microstructure images showing subtle effect of the varied synthesis parameter of graphene additive % from 0.01% to 0.025% and 0.05%. This allows domain scientists to visualize and understand how changes in material attributes, synthesis/ processing conditions impact the sample microstructure features which in turn determine its properties and thus can further be optimized. Further applications of AI coupled with multi-criteria multi-objective property optimization, optimal design of experiments and active learning as well as investigation of the explainability of the models built will be subjects of future research.

Acknowledgements

We thank Emily Wolbeck, Cindy Barrera-Martinez, Amy Langhorst, Haibo Zhao for interesting discussions of the mechanical characterization and microstructure images data for this work.

References

- Alasti Bonab, S.; Moghaddas, J.; and Rezaei, M. 2019. In-situ synthesis of silica aerogel/polyurethane inorganic-organic hybrid nanocomposite foams: Characterization, cell microstructure and mechanical properties. *Polymer*, 172: 27–40.
- Gola, J.; Britz, D.; Staudt, T.; Winter, M.; Schneider, A. S.; Ludovici, M.; and Mücklich, F. 2018. Advanced microstructure classification by data mining methods. *Computational Materials Science*, 148: 324–335.
- Gómez-Bombarelli, R.; Wei, J. N.; Duvenaud, D.; Hernández-Lobato, J. M.; Sánchez-Lengeling, B.; Sheberla, D.; Aguilera-Iparraguirre, J.; Hirzel, T. D.; Adams, R. P.; and Aspuru-Guzik, A. 2018. Automatic Chemical Design Using a Data-Driven Continuous Representation of Molecules. *ACS Central Science*, 4(2): 268–276. PMID: 29532027.
- He, K.; Zhang, X.; Ren, S.; and Sun, J. 2016. Deep Residual Learning for Image Recognition. In *2016 IEEE Conference on Computer Vision and Pattern Recognition (CVPR)*, 770–778.
- He, Z.; Zuo, W.; Kan, M.; Shan, S.; and Chen, X. 2019. AttGAN: Facial Attribute Editing by Only Changing What You Want. *IEEE Transactions on Image Processing*, 28(11): 5464–5478.
- Himanan, L.; Geurts, A.; Foster, A. S.; and Rinke, P. 2019. Data-Driven Materials Science: Status, Challenges, and Perspectives. *Advanced Science*, 6(21): 1900808.
- Hiszpanski, A. M.; Gallagher, B.; Chellappan, K.; Li, P.; Liu, S.; Kim, H.; Han, J.; Kailkhura, B.; Buttler, D. J.; and Han, T. Y.-J. 2020. Nanomaterial Synthesis Insights from Machine Learning of Scientific Articles by Extracting, Structuring, and Visualizing Knowledge. *Journal of Chemical Information and Modeling*, 60(6): 2876–2887. PMID: 32286818.
- Holm, E. A. 2019. In defense of the black box. *Science*, 364(6435): 26–27.
- Iwasaki, Y.; Sawada, R.; Stanev, V.; Ishida, M.; Kirihara, A.; Omori, Y.; Someya, H.; Takeuchi, I.; Saitoh, E.; and Shinichi, Y. 2019. Materials development by interpretable machine learning. arXiv:1903.02175.
- Jha, D.; Choudhary, K.; Tavazza, F.; Liao, W.-K.; Choudhary, A.; Campbell, C.; and Agrawal, A. 2019. Enhancing materials property prediction by leveraging computational and experimental data using deep transfer learning. *Nat Commun*, 10(1): 5316.
- Krizhevsky, A.; Sutskever, I.; and Hinton, G. E. 2012. ImageNet classification with deep convolutional neural networks. *Advances in neural information processing systems*, 25: 1097–1105.
- Kucheyev, S. O.; Baumann, T. F.; Cox, C. A.; Wang, Y. M.; Satcher, J. H.; Hamza, A. V.; and Bradby, J. E. 2006. Nanoengineering mechanically robust aerogels via control of foam morphology. *Applied Physics Letters*, 89(4): 041911.
- Liu, S.; Kailkhura, B.; Zhang, J.; Hiszpanski, A. M.; Robertson, E.; Loveland, D.; and Han, T. Y.-J. 2020. Explainable Deep Learning for Uncovering Actionable Scientific Insights for Materials Discovery and Design. arXiv:2007.08631.
- Luo, G.; Gu, X.; Zhang, J.; Zhang, R.; Shen, Q.; Li, M.; and Zhang, L. 2017. Microstructural, mechanical, and thermal-insulation properties of poly(methyl methacrylate)/silica aerogel bimodal cellular foams. *Journal of Applied Polymer Science*, 134(6).
- Pun, G. P. P.; Batra, R.; Ramprasad, R.; and Mishin, Y. 2019. Physically informed artificial neural networks for atomistic modeling of materials. *Nature Communications*, 10(1): 2339.
- Rickman, J. M.; Balasubramanian, G.; Marvel, C. J.; Chan, H. M.; and Burton, M.-T. 2020. Machine learning strategies for high-entropy alloys. *Journal of Applied Physics*, 128(22): 221101.
- Schwalbe-Koda, D.; and Gómez-Bombarelli, R. 2020. *Generative Models for Automatic Chemical Design*, 445–467. Cham: Springer International Publishing. ISBN 978-3-030-40245-7.
- Selvaraju, R. R.; Cogswell, M.; Das, A.; Vedantam, R.; Parikh, D.; and Batra, D. 2017. Grad-CAM: Visual Explanations from Deep Networks via Gradient-Based Localization. In *2017 IEEE International Conference on Computer Vision (ICCV)*, 618–626.
- Stein, H. S.; and Gregoire, J. M. 2019. Progress and prospects for accelerating materials science with automated and autonomous workflows. *Chem. Sci.*, 10: 9640–9649.
- Wu, S.; Kondo, Y.; Kakimoto, M.-a.; Yang, B.; Yamada, H.; Kuwajima, I.; Lambard, G.; Hongo, K.; Xu, Y.; Shiomi, J.; Schick, C.; Morikawa, J.; and Yoshida, R. 2019. Machine-learning-assisted discovery of polymers with high thermal conductivity using a molecular design algorithm. *npj Computational Materials*, 5(1): 66.
- Xie, T.; and Grossman, J. C. 2018. Crystal Graph Convolutional Neural Networks for an Accurate and Interpretable Prediction of Material Properties. *Phys. Rev. Lett.*, 120: 145301.
- Yang, K.; Goldman, S.; Jin, W.; Lu, A.; Barzilay, R.; Jaakkola, T.; and Uhler, C. 2020. Improved Conditional Flow Models for Molecule to Image Synthesis. arXiv:2006.08532.
- Zachary D., A. e. a., Kiziltas. 2019. Flexible Polyurethane Foams for Closed Loop Recycling Of Additive Manufacturing Waste. Ford internal technical report. Forthcoming.
- Zhuo, Y.; Mansouri Tehrani, A.; Oliynyk, A. O.; Duke, A. C.; and Brgoch, J. 2018. Identifying an efficient, thermally robust inorganic phosphor host via machine learning. *Nature Communications*, 9(1): 4377.